Sorption of zinc by novel pH-sensitive hydrogels based on chitosan, itaconic acid and methacrylic acid

Nedeljko B. Milosavljević [a], Mirjana Đ. Ristić [a], Aleksandra A. Perić-Grujić [a], Jovanka M. Filipović [a], Svetlana B. Štrbac [b], Zlatko Lj. Rakočević [c], Melina T. Kalagasidis Krušić [a],*

[a] Faculty of Technology and Metallurgy, University of Belgrade, Karnegijeva 4, 11120 Belgrade, Serbia
[b] ICTM-Institute of Electrochemistry, University of Belgrade, P.O.B. 815, 11001 Belgrade, Serbia
[c] INS Vinča, Laboratory for Atomic Physics, University of Belgrade, P.O.B. 522, Mike Alasa 12-14, 11001 Belgrade, Serbia

ABSTRACT

Novel pH-sensitive hydrogels based on chitosan, itaconic acid and methacrylic acid were applied as adsorbents for the removal of Zn^{2+} ions from aqueous solution. In batch tests, the influence of solution pH, contact time, initial metal ion concentration and temperature was examined. The sorption was found pH dependent, pH 5.5 being the optimum value. The adsorption process was well described by the pseudo-second order kinetic. The hydrogels were characterized by spectral (Fourier transform infrared—FTIR) and structural (SEM/EDX and atomic force microscopy—AFM) analyses. The surface topography changes were observed by atomic force microscopy, while the changes in surface composition were detected using phase imaging AFM. The negative values of free energy and enthalpy indicated that the adsorption is spontaneous and exothermic one. The best fitting isotherms were Langmuir and Redlich–Peterson and it was found that both linear and nonlinear methods were appropriate for obtaining the isotherm parameters. However, the increase of temperature leads to higher adsorption capacity, since swelling degree increased with temperature.

© 2011 Elsevier B.V. All rights reserved.

1. Introduction

Trace elements, especially heavy metals, are currently pollutants of great concern, due to increased awareness of their potential hazardous effects. Released in environment mostly by industrial plants or mining activities, they pollute soil, surface waters, sediments, as well as ground water. Many industrial activities generate heavy metal contaminated wastewaters with very diverse compositions that pose serious environmental risks if not treated [1]. As stable and persistent, they may accumulate in living organisms, enter and become concentrated in a food chain. Even low concentrations of heavy metals have damaging effects to men and animals because there is no good mechanism for their elimination from the body [2].

Zinc as an essential trace element is crucial to survival and health maintenance of living organisms. However, insufficient, as well as excessive intake, can cause disease and toxicity. Zinc human toxicity can occur in both acute and chronic forms. Acute adverse effects of high zinc intake include nausea, vomiting, loss of appetite, abdominal cramps, diarrhea, and headaches [3]. Also, it should be

emphasized that zinc and its salts have high acute and chronic toxicity to aquatic life in polluted waters.

Zinc has many commercial applications such as coatings to prevent rust, in dry-cell batteries, in many alloys (such as brass and bronze), and in the production of die castings. Compounds of zinc are used in the manufacture of paints, plastics, rubber, dyes, wood preservatives and cosmetics. Due to its high production and application, zinc can be found in emission, effluents, sludges and waste.

Recently, articles dealing with Zn^{2+} separation from synthetic wastewater have been published: removal by simultaneous sulfate reduction and zinc precipitation in a single gas-lift bioreactor [4]; biosorption by orange waste in batch and packed-bed systems [5]; removal by using hybrid precursor of silicon and carbon [6]; sorption by the Serbian natural clinoptilolite [7] and separation by extractant-impregnated organogels [8]. Since clay minerals are already known to be efficient sorbent of various pollutants [9–18], bentonite was also used for the Zn^{2+} removal from aqueous solution [19,20].

Novel pH-sensitive hydrogels based on chitosan, itaconic acid and methacrylic acid were synthesised as a combination of natural and synthetic polymers with improved mechanical properties and tunable swelling [21]. One of these materials was applied as efficient adsorbent of Cd^{2+} ions from aqueous solution [22]. In the present study the same hydrogel was used as a sorbent for Zn^{2+}

* Corresponding author. Tel.: +381 11 3303730; fax: +381 11 3370387.
 E-mail address: meli@tmf.bg.ac.rs (M.T. Kalagasidis Krušić).

ions and also two other hydrogels based on chitosan, itaconic acid and methacrylic acid were examined.

The objective of this research was the investigation and characterization of new pH-sensitive chitosan based materials as a sorbent for Zn^{2+} ion removal from synthetic wastewater solution. SEM/EDX, FTIR and AFM analyses were applied for their characterization. The influence of different variables like pH, temperature, contact time and initial concentration on the Zn^{2+} ions uptake was examined.

2. Materials and methods

2.1. Materials and methods

The synthesis and characterization of pH-sensitive hydrogels based on chitosan (Ch), itaconic acid (IA) and methacrylic acid (MAA) have been already described [21]. In this research the hydrogels Ch/IA/MAA-1, Ch/IA/MAA-2 and Ch/IA/MAA-3 were examined as sorbents for Zn^{2+} ions. Chitosan Ch/IA/MAA weight ratios were 1:1.56:10 (Ch/IA/MAA-1 and Ch/IA/MAA-2) and 1:1.56:7.5 (Ch/IA/MAA-3). The redox pair KPS ($K_2S_2O_8$) and KPyS ($K_2S_2O_7$), both 0.2 wt.% with respect to the total weight of the reaction mixture, was used as initiator and N,N′-methylenebisacrylamide (MBA) as the crosslinking agent. The MBA concentration was 0.2 wt.% for Ch/IA/MAA-1 and Ch/IA/MAA-3 and 0.4 wt.% for Ch/IA/MAA-2.

Zinc stock solution (1000 mg/L) was prepared by dissolving a calculated amount of $Zn(NO_3)_2 \cdot 6H_2O$ (Merck, p.a.). Double distilled deionized water was used through the research.
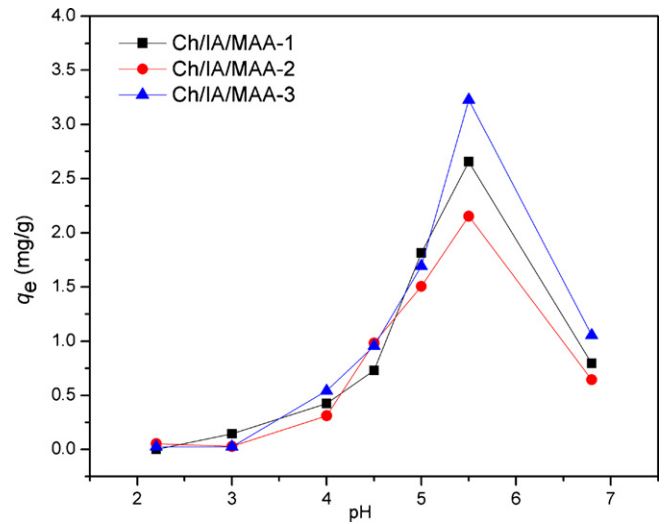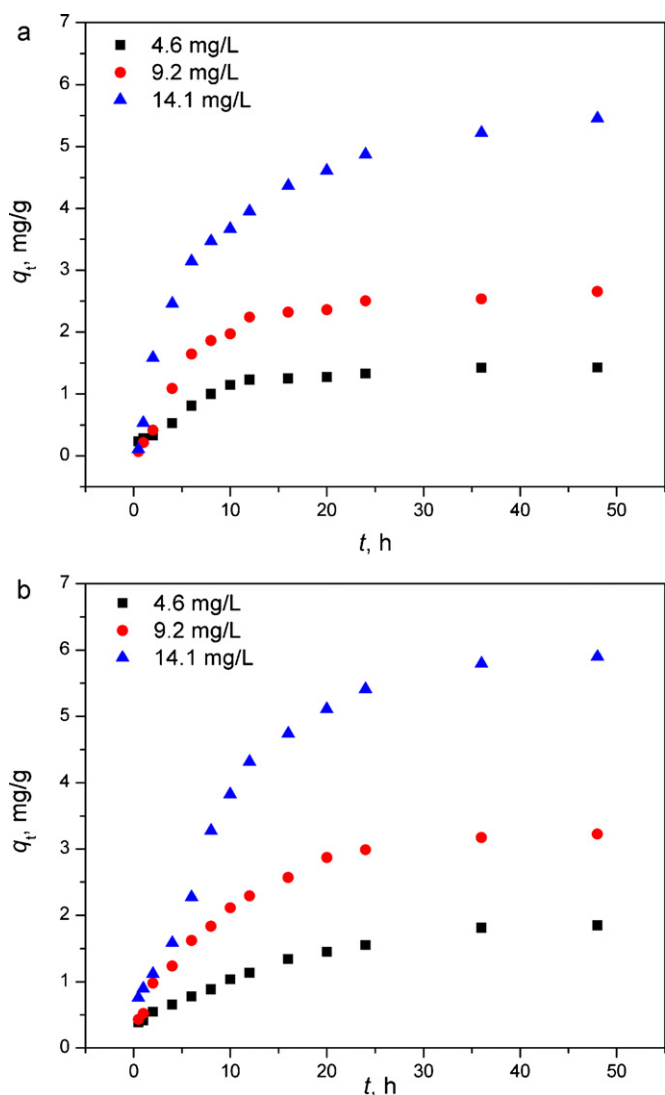

Fig. 1. Effect of pH on Zn^{2+} ion adsorption onto Ch/IA/MAA hydrogels. Amount of hydrogel 0.035 g; $C_o = 10$ mg/L; temperature 25 °C; contact time 48 h.

All batch kinetics experiments were carried out by mixing 0.035 g of hydrogel with 50 mL of aqueous solution of Zn^{2+} ions. The adsorbate concentration (4.6, 9.2 and 14.1 mg/L), pH, adsorption time (0.5–48 h) and temperature (25 °C, 37 °C and 45 °C) were varied. The pH of the aqueous phase was adjusted within

Table 1
Characteristic parameters of the applied kinetic models and the correlation coefficients.

Sample	Parameters	$q_{e,exp}$ (mg/g)	Pseudo-first order model linear method			Pseudo-second order model linear method		
			k_1 (min^{-1})	$q_{e,cal}$ (mg/g)	R^2	k_2 (g/mg min)	$q_{e,cal}$ (mg/g)	R^2
Ch/IA/MAA-1	Initial Zn(II) concentration; sample dose: 0.035 g; pH 5.5; $V = 50$ mL; $t = 25$ °C							
	4.6	1.43	2.66	1.65	0.9014	2.55	1.60	0.9885
	9.2	2.65	1.57	2.02	0.9047	1.24	2.93	0.9958
	14.1	5.46	1.42	4.48	0.9821	0.56	6.11	0.9994
	Temperature (°C); C_0: 9.2 mg/L; sample dose: 0.035 g; pH 5.5; $V = 50$ mL;							
	25	2.65	1.57	2.02	0.9047	1.24	2.93	0.9958
	37	3.97	1.16	2.38	0.9741	1.35	4.10	0.9934
	45	6.34	1.38	2.98	0.9884	1.51	7.37	0.9900
Ch/IA/MAA-3	Initial Zn(II) concentration; sample dose: 0.035 g; pH 5.5; $V = 50$ mL; $t = 25$ °C							
	4.6	1.84	1.56	1.88	0.9276	1.34	1.82	0.9639
	9.2	3.23	1.54	2.51	0.9897	0.91	3.68	0.9921
	14.1	5.90	1.42	4.48	0.9921	0.41	7.05	0.9934
	Temperature (°C); C_0: 9.2 mg/L; sample dose: 0.035 g; pH 5.5; $V = 50$ mL;							
	25	3.23	1.54	2.51	0.9897	0.91	3.68	0.9921
	37	4.64	1.42	2.41	0.9654	1.03	5.02	0.9980
	45	5.53	1.14	3.07	0.9852	1.06	5.66	0.9924

Sample	Parameters	$q_{e,exp}$ (mg/g)	Pseudo-first order model non-linear method			Pseudo-second order model non-linear method		
			k_1 (min^{-1})	$q_{e,cal}$ (mg/g)	R^2	k_2 (g/mg min)	$q_{e,cal}$ (mg/g)	R^2
Ch/IA/MAA-1	Initial Zn(II) concentration; sample dose: 0.035 g; pH 5.5; $V = 50$ mL; $t = 25$ °C							
	4.6	1.43	2.15	1.68	0.9868	2.49	1.40	0.9978
	9.2	2.65	1.84	3.15	0.9881	1.18	2.60	0.9985
	14.1	5.46	1.33	6.16	0.9831	0.85	5.23	0.9946
	Temperature (°C); C_0: 9.2 mg/L; sample dose: 0.035 g; pH 5.5; $V = 50$ mL;							
	25	2.65	1.14	3.15	0.9891	1.33	2.60	0.9966
	37	3.97	1.28	3.55	0.9873	1.42	3.77	0.9944
	45	6.34	1.47	5.85	0.9857	1.49	6.12	0.9942
Ch/IA/MAA-3	Initial Zn(II) concentration; sample dose: 0.035 g; pH 5.5; $V = 50$ mL; $t = 25$ °C							
	4.6	1.84	1.09	2.20	0.9746	1.21	1.80	0.9912
	9.2	3.23	1.12	3.82	0.9890	1.14	3.17	0.9910
	14.1	5.90	1.10	6.58	0.9874	0.75	6.00	0.9964
	Temperature (°C); C_0: 9.2 mg/L; sample dose: 0.035 g; pH 5.5; $V = 50$ mL;							
	25	3.23	1.44	3.82	0.9800	1.00	3.17	0.9910
	37	4.64	1.28	4.09	0.9771	1.19	4.59	0.9986
	45	5.53	1.05	4.45	0.9862	1.16	5.62	0.9987

k_1—the rate constant of pseudo-first order model, k_2—the rate constant of pseudo-second order model.

Fig. 2. Sorption kinetics of Ch/IA/MAA-1 (a) and Ch/IA/MAA-3 (b) hydrogel at different initial Zn²⁺ concentrations. Amount of sorbent 0.035 g; volume of the solution 50 mL; initial pH 5.5; temperature 25 °C; contact time 0.5–48 h.

Table 2
Isotherm parameters obtained using the linear and non-linear method for the adsorption of Zn^{2+} ions onto the Ch/IA/MAA-3 hydrogel at 25 °C, 37 °C and 45 °C at different temperatures.

Parameter	25 °C	37 °C	45 °C
Langmuir linear			
q_{max} (mg/g)	105.5	109.4	111.6
K_L (L/g)	4.50	5.3	7.3
R^2	0.9955	0.9967	0.9933
Freundlich linear			
K_F (mg/g)(L/mg)$^{1/n}$	2.02	2.51	3.72
n	1.72	1.78	1.94
R^2	0.9875	0.9892	0.9887
Redlich Peterson linear			
A (L/g)	0.629	0.865	0.887
B (L/mg)^g	0.027	0.021	0.023
g	0.776	0.848	0.824
R^2	0.9924	0.9975	0.9968
Langmuir nonlinear			
q_{max} (mg/g)	104.2	107.9	117.5
K_L (L/g)	4.1	6.5	8.2
R^2	0.9920	0.9959	0.9947
Freundlich nonlinear			
K_F (mg/g)(L/mg)$^{1/n}$	2.1	2.9	4.2
n	1.75	1.97	2.02
R^2	0.9833	0.9824	0.9742
Redlich Peterson nonlinear			
A (L/g)	0.653	0.712	0.980
B (L/mg)^g	0.031	0.019	0.021
g	0.755	0.833	0.866
R^2	0.9966	0.9983	0.9982

q_{max}—maximum sorption capacity; K_L—Langmuir constant; K_F—Freundlich isotherm constant; n—Freundlich exponent; A, B, g—Redlich–Peterson isotherm constants.

3. Results and discussion

3.1. Sorption studies

Experiments with initial pH ranging from 2.2 to 6.8 and Zn^{2+} initial concentration of 10 mg/L were carried out by adding 0.035 g of hydrogel (Ch/IA/MAA-1, Ch/IA/MAA-2 and Ch/IA/MAA-3) into 50 mL of zinc-nitrate solution.

The Zn^{2+} ion adsorption is highly dependent on solution pH for all examined hydrogels, as shown in Fig. 1. The maximum adsorption of Zn^{2+} ions onto all three adsorbents occurred at pH 5.5. The pH of aqueous solution is very important parameter for Zn^{2+} ion sorption on Ch/IA/MAA hydrogel because it affects the metal chemistry in the solution and the hydrogel properties like swelling and charge of the functional groups, as well. An increase of solution pH from 2.2 to 5.5 substantially increases the metal ion adsorption and then declines with a further increase of pH. Depending on the solution pH, different metallic species are present (Zn^{2+}, $Zn(OH)^+$, $Zn(OH)_2$(s), etc.) [23] and at pH 2.2–5 the Zn^{2+} ions are the main species in the solution. In the pH range 2.2–5.5 the pH dependence of Zn^{2+} ion adsorption on the examined hydrogels can largely be related to swelling and charge of hydrogel functional groups because at pH 5.45 all acid groups become ionized. Also, electrostatic repulsive forces between anions lead to a marked increase of swelling [21]. At pH > 6 hydrogen bonding between amine and hydroxyl groups takes place and the shrinkage of the gels occurs. Also, few authors performed Zn^{2+} ion adsorption at pH about 6 to avoid any possible precipitation [7,24].

The lower adsorption capacity of Ch/IA/MAA-2 hydrogel (Fig. 1) can be attributed to its lower swelling degree, compared with other two hydrogels, being a consequence of the increased MBA concentration (0.4%). It has been shown that with the increase of the MBA concentration increases the extent of crosslinking and the degree
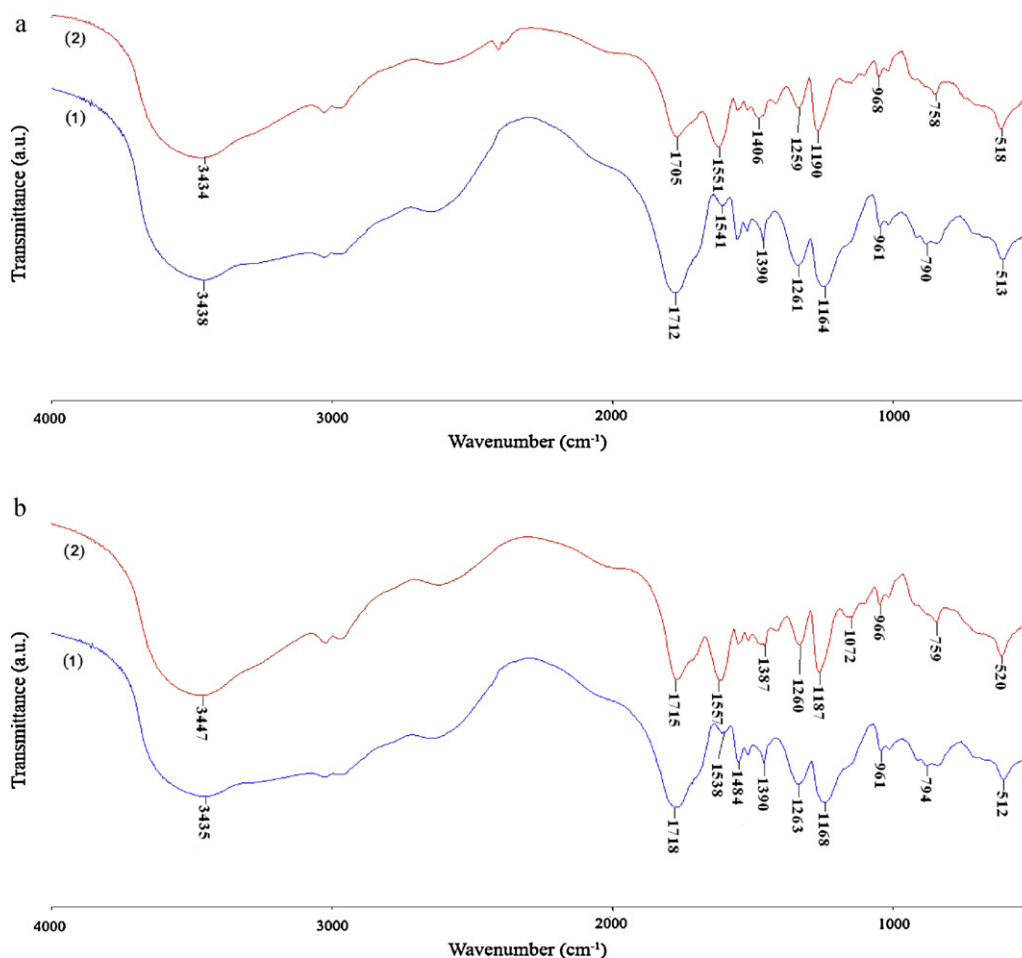
the range 2.2–6.8. The flasks were agitated on a thermostatted mechanical shaker (WNB-14, Memmert). The concentration of Zn^{2+} ion in solution was determined by ICP-MS Agilent Technologies 7500ce system. Adsorption isotherms were studied over a large Zn^{2+} initial concentration range, from 4.6 to 660 mg/L at pH 5.5.

Fourier transform infrared (FTIR) spectra of unloaded and loaded hydrogel were obtained using a Bomem MB 100 FTIR spectrophotometer.

The morphology of the prepared hydrogel was investigated using SEM/EDX, on a JEOL JSM-5800 scanning electron microscope.

Multimode quadrex SPM with Nanoscope IIIe controller (Veeco Instruments, Inc.), operated under ambient conditions was used to simultaneously acquire surface topography and phase images. Standard AFM tapping mode was explored using a commercial Veeco RTESP AFM probe. All measurements were performed in one series using the same cantilever and with the same value of the drive amplitude set at 32.2 mV. The drive frequency was 246.830 kHz, while the amplitude set point was 2.7 ± 0.1 V.

Fig. 3. FTIR spectra of the (a) Ch/IA/MAA-1 and (b) Ch/IA/MAA-3 hydrogel samples before (1) and after (2) Zn²⁺ ions adsorption.

of swelling decreases, at all pH values [21]. Higher amount of Zn^{2+} ions is adsorbed by Ch/IA/MAA-3 (Fig. 1) which has lower swelling degree and lower MAA content than Ch/IA/MAA-1 hydrogel [21].

The subsequent experiments were performed with two hydrogels, Ch/IA/MAA-1 and Ch/IA/MAA-3 at pH 5.5.

The results of kinetic experiments are presented in Fig. 2(a and b). The amount of Zn (mg) adsorbed per gram of Ch/IA/MAA hydrogel, q_t, versus contact time (0–48 h) for different initial metal ion concentrations is shown. For both hydrogels the increase of the initial concentration, as well as contact time, leads to an increase in the amount of metal ion adsorbed; the Ch/IA/MAA-3 exhibits a little bit higher sorption capacity. Due to similar properties of examined materials for both of them equilibrium is reached within 40 h. The contact time of 48 h was chosen for the further sorption experiments.

In order to investigate the rate constant, adsorption process was analyzed using two the most widely applied kinetic models in sorption processes, pseudo-first model proposed by Lagergren [25] and pseudo-second order proposed by Ho and McKay [26]. The characteristic parameters of the studied kinetic models and their corresponding correlation coefficients are presented in Table 1. Judging from the correlation coefficients, R^2, the pseudo-second order model fits better with the experimental data than pseudo-first model for both hydrogels and also the calculated q_e values ($q_{e,cal}$) obtained with pseudo-second order kinetic model are more consistent with the experimental q_e values ($q_{e,exp}$). Obviously, the adsorption process of Zn^{2+} ions on Ch/IA/MAA-1 and Ch/IA/MAA-3 hydrogels can be well described by the pseudo-second order model. Moreover, for the system studied at increased temperatures

the pseudo-second order model provides better correlation of the experimental data, comparing with the pseudo-first model.

3.2. Characterization of hydrogels

Fig. 3 shows the FTIR spectra of Ch/IA/MAA-1 and Ch/IA/MAA-3 hydrogels, free and metal-loaded. The wide absorption band at $\sim$3435 cm^{-1} is characteristic of the N–H and –OH stretching vibrations. The intensity of this band decreases in the FTIR spectrum of zinc-loaded hydrogels indicating that these two groups are possibly involved in the adsorption. Also, the FTIR spectra of Ch/IA/MAA-1 showed that the C=O stretching vibration from carboxylic groups obviously weakened after adsorption and the strong absorption band at 1712 cm^{-1} (Fig. 3a-1) shifted to the lower wave number, 1705 cm^{-1} (Fig. 3a-2) in the metal loaded spectrum. Similar pattern was observed for Ch/IA/MAA-3 hydrogel where absorption band at 1718 cm^{-1} (Fig. 3b-1) shifted to 1715 cm^{-1} (Fig. 3b-2) after zinc adsorption, indicating that the same groups are involved in adsorption. The absorption band at $\sim$1540 cm^{-1}, assigned to the ionic interaction between Ch and the acids, as well as the absorption band at $\sim$1165 cm^{-1}, assigned to the deformation absorption bands of –OH groups, were enhanced and shifted to higher wave numbers after zinc adsorption, for both hydrogels. On the basis of the FTIR spectra of unloaded and loaded hydrogel it seems that –NH$_2$, –OH and –COOH groups are involved in Zn^{2+} ion bonding to the hydrogels.

The SEM images of Ch/IA/MAA-1 and Ch/IA/MAA-3 hydrogels, before and after adsorption are shown in Fig. 4a′ Fig. 4 shows that the structure of the unloaded Ch/IA/MAA-1 hydrogel is highly
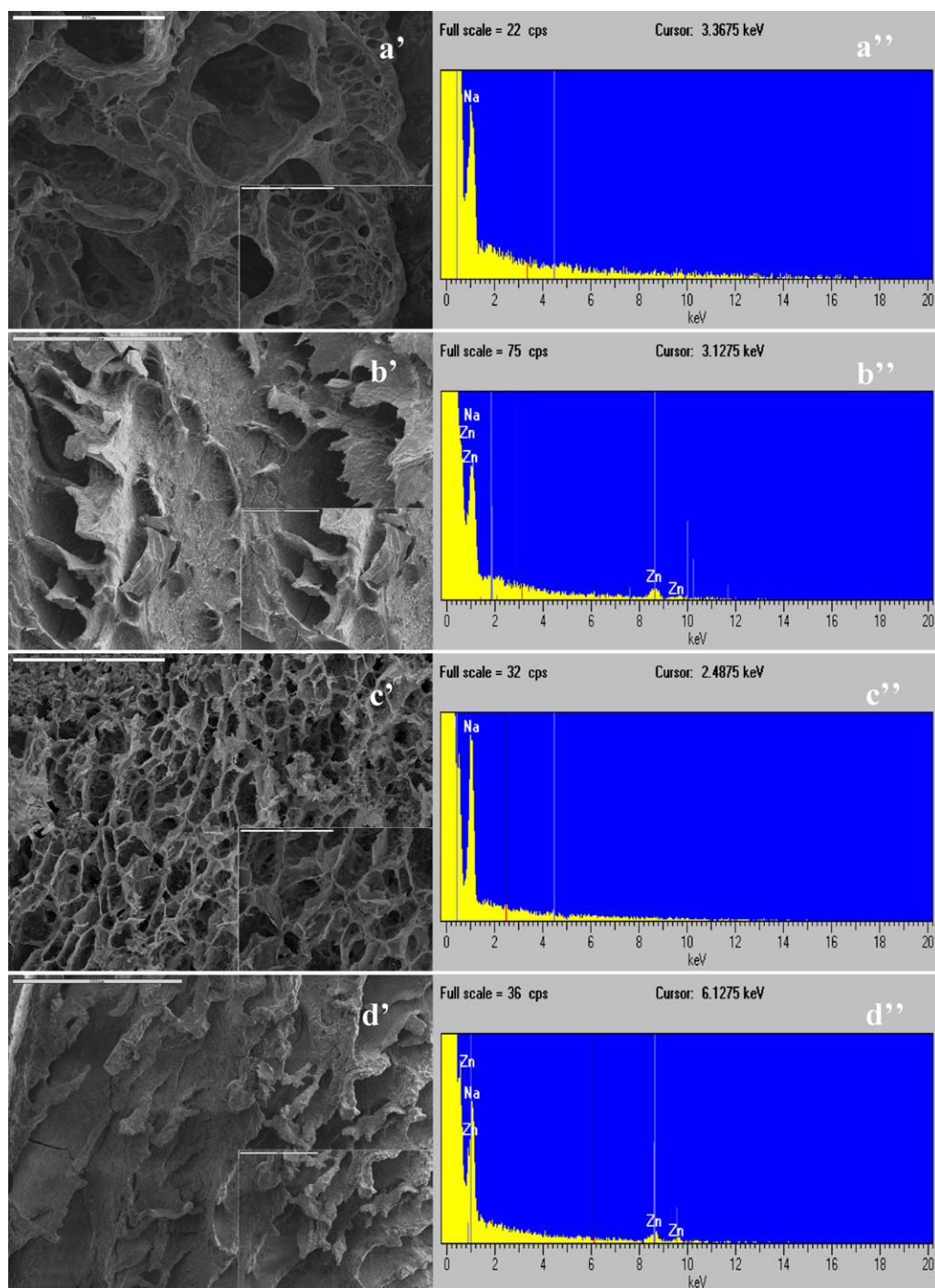
Fig. 4. (a′) SEM micrograph 'bar' 500 μm, 90×; zoom 'bar' 200 μm, 300× and (a″) EDX spectra of intact Ch/IA/MAA-1 sample. (b′) SEM micrograph 'bar' 200 μm, 250×; zoom 'bar' 200 μm, 500× and (b″) EDX spectra of Ch/IA/MAA-1 sample after loading with zinc nitrate solution (324.8 mg/L). (c′) SEM micrograph 'bar' 500 μm, 90×; zoom 'bar' 200 μm, 300× and (c″) EDX spectra of intact Ch/IA/MAA-3 sample. (d′) SEM micrograph 'bar' 200 μm, 250×; zoom 'bar' 100 μm, 500× and (d″) EDX spectra of Ch/IA/MAA-3 sample after loading with zinc nitrate solution (324.8 mg/L).

porous while from Fig. 4b′ is obvious that zinc ions adsorption causes significant changes in its structure. Typical EDX spectra of the unloaded Ch/IA/MAA-1 hydrogel and the hydrogel after zinc adsorption are presented in Fig. 4(a″ and b″). EDX was employed to confirm whether the electron dense part on the hydrogel is made up of Zn^{2+} ions. The existence of zinc ions on the Ch/IA/MAA-1 hydrogel is confirmed by EDX spectra; while the EDX spectrum for the intact hydrogel did not show the characteristic peak of zinc, the EDX spectrum of zinc-loaded hydrogel showed clearly the peak of zinc, intensity of which is proportional to the metal concentration.

On Fig. 4c′ the unloaded highly porous Ch/IA/MAA-3 hydrogel is shown, and on Fig. 4d′ the same hydrogel after zinc adsorption, which caused significant changes in its structure. EDX spectras of the unloaded Ch/IA/MAA-3 hydrogel and the same hydrogel after zinc adsorption are presented in Fig. 4(c″ and d″).

Hydrogel morphology is obviously dependent on the MAA content, and larger pores are observed for the Ch/IA/MAA-1 hydrogel. The surface of Ch/IA/MAA-3 hydrogel was more porous and provided larger surface area for Zn^{2+} ion adsorption. This is confirmed by EDX spectrum of zinc-loaded hydrogels (Fig. 4b′ and b″) where

intensity of the peak of zinc is higher for Ch/IA/MAA-3 hydrogel comparing with Ch/IA/MAA-1 hydrogel.

On the basis of the results obtained, Ch/IA/MAA-3 hydrogel was chosen for adsorption isotherm experiment.

3.3. Adsorption isotherms

The experimental equilibrium isotherms for adsorption of Zn^{2+} ions on Ch/IA/MAA-3 hydrogel at different temperatures are presented at Fig. 5. The equilibrium adsorption data were subjected to the three widely used isotherms, Langmuir and Freundlich, as two parameter isotherms, and Redlich–Peterson, as a three parameter model. Linear and nonlinear methods were used in order to obtain the best fitting of the isotherms; the parameters of the adsorption isotherms are presented in Table 2.

The linear and nonlinear correlation coefficients for the Langmuir and Redlich–Peterson model are higher, than those of the Freundlich model, at all temperatures, thus indicating that the Langmuir and the Redlich–Peterson isotherms best fitted for the adsorption of Zn^{2+} ions on Ch/IA/MAA-3 hydrogel under the concentration range studied. The prediction of the adsorption process can be performed using both linear and nonlinear method since the calculated isotherm parameters obtained using these methods were similar.

The studies of the temperature effect on the Zn^{2+} ions adsorption by Ch/IA/MAA-3 hydrogel were carried out at three different temperatures (25 °C, 37 °C and 45 °C) at optimum pH value of 5.5, contact time 48 h and adsorbent dosage level of 0.035 g.

The Langmuir constant K_L is used in the following equation to determine the Gibbs free energy change of adsorption, ΔG, at different temperatures:

$$\Delta G = -RT \ln K_L \qquad (1)$$

where R is the universal gas constant (8.314 J/mol K) and T is the temperature.

The thermodynamic parameters, enthalpy change (ΔH) and entropy change (ΔS), are calculated from the values of the slope and intercept of a plot $\ln K_L$ versus $1/T$ (Eq. (2)).

$$\ln K_L = \frac{\Delta S}{R} - \frac{\Delta H}{RT} \qquad (2)$$

The negative values of ΔG obtained (−20.84, −22.10 and −23.52 kJ/mol at 25 °C, 37 °C and 45 °C, respectively) confirm the feasibility of the process and the spontaneous nature of Zn^{2+} ion adsorption on Ch/IA/MAA-3 hydrogel. Also the value of ΔG becomes more negative with the increase of temperature.

The values obtained for the enthalpy change, ΔH, and the entropy change, ΔS, were −18.26 kJ/mol and 130.93 J/mol K, respectively. Even the negative value of ΔH indicates that the adsorption reaction is exothermic, the results obtained showed that with the increase of temperature, the process becomes more spontaneous and the adsorption capacity also increased. Namely, temperature also has significant influence on the hydrogel swelling, as shown in Fig. 6. As the swelling values exhibit great difference in the investigated temperature range, increased sorption capacity is attributed to the higher degree of swelling at elevated temperatures.

The positive value of ΔS suggests some structural changes during Zn^{2+} ion adsorption and Ch/IA/MAA-3 hydrogel interactions. Namely, it has been previously concluded that some water structural break-down in the adsorption process could be expected [27]. Probably the size of hydration sphere of Zn^{2+} ions, hydration energy and structure of the hydrogel contribute to the obtained ΔS value.
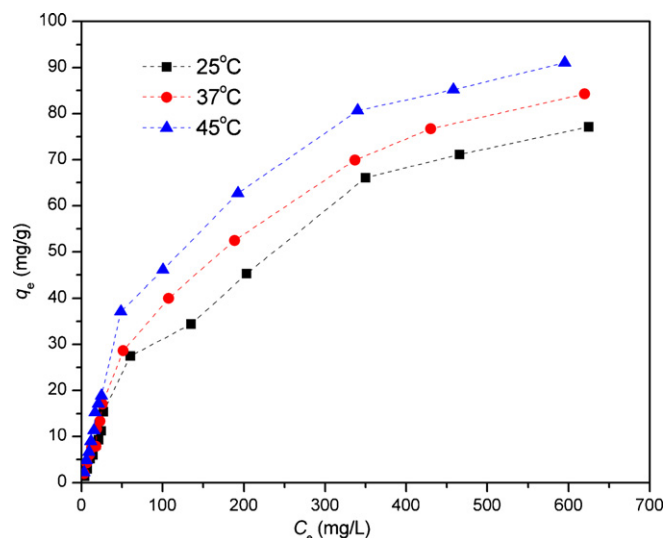

Fig. 5. Adsorption equilibrium isotherms of Ch/IA/MAA-3 hydrogel. Amount of hydrogel 0.035 g; pH 5.5; contact time 48 h.

3.4. AFM surface topography and phase images

Surface topography images were acquired using tapping-mode atomic force microscopy (AFM), while simultaneously recorded phase AFM images were used to detect the changes in surface chemical composition after Zn^{2+} ions were adsorbed by the reference sample from solutions containing different Zn concentrations.

Characteristic three dimensional (3D) surface topography and phase AFM images (500 nm × 500 nm) of the reference sample and of ones modified by absorbed Zn, are presented in Fig. 7. Grains of various sizes randomly aggregated can be seen in Fig. 7a. Due to the contrast enhancement in phase images, particular grains are clearly highlighted in Fig. 7b.

Upon Zn adsorption, a significant change in surface topography is obtained. Grains of the reference sample are agglomerated giving thus flattened domains of the Zn/ref surface, as illustrated in Fig. 7c. Another consequence of the agglomeration is the appearance of very large grains, displacement of which leaves huge holes behind. Presence of displaced grains and holes on the surface in the zinc containing phase is indicated by a light contrast in phase image, Fig. 7d. The agglomeration is more pronounced resulting in
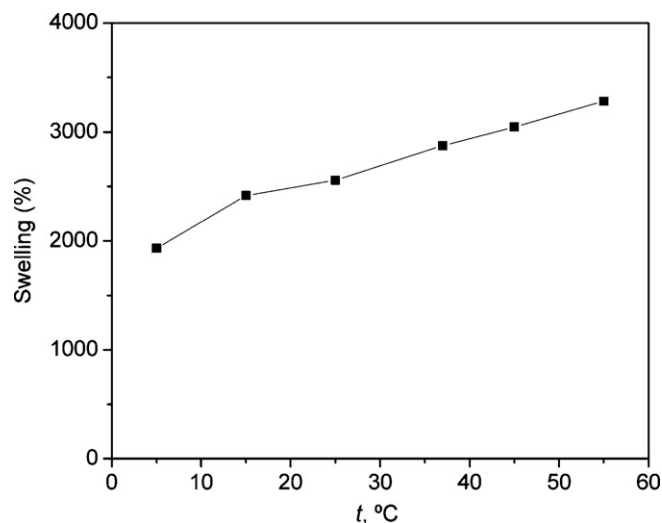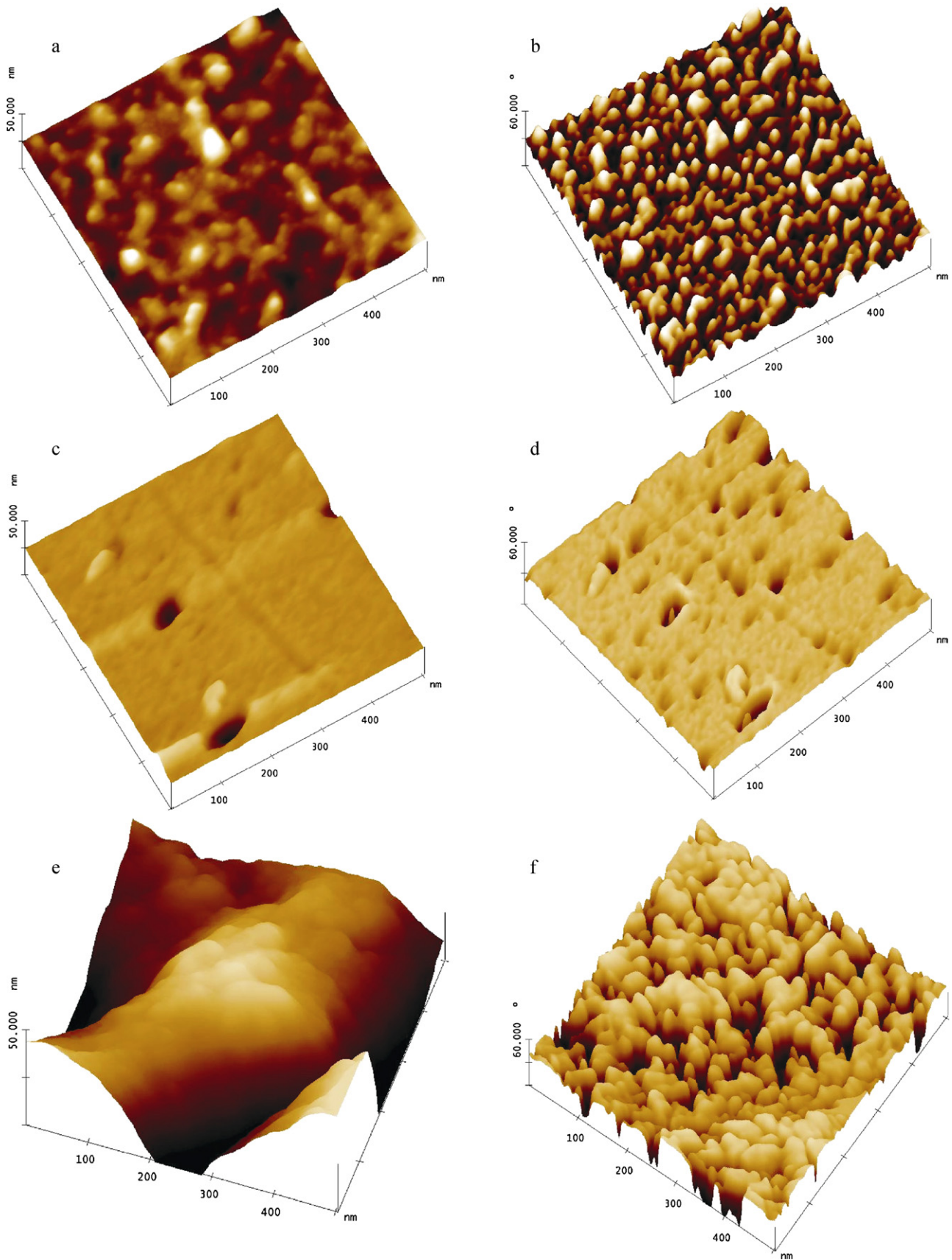

Fig. 6. The effect of temperature on the swelling of Ch/IA/MAA-3 hydrogel.

Fig. 7. AFM images (500 nm × 500 nm) showing: (a) the morphology of the reference sample and (b) the corresponding phase image; (c) the morphology of the same sample containing Zn^{2+} ions, after adsorption from the Zn^{2+} ion solution (initial concentration 80 mg/L) and d) the corresponding phase image; (e) the same sample containing Zn^{2+} ions adsorbed (initial concentration 320 mg/L) and (f) the corresponding phase image. For surface morphology images z-range is 10 nm, while for phase images z-range is 60°.

Table 3
Maximum adsorption capacity of different adsorbents for Zn^{2+} ions at 25 °C.

Adsorbent	q_{max} (mg/g)	Reference
Natural bentonite	68.5	[20]
Orange waste	34.5	[5]
Hybrid precursors of silicon and carbon	28.76	[6]
Serbian natural clinoptilolite	12.0	[7]
pH sensitive hydrogel	110[a]	[28]
Chelating Polymeric Hydrogel	83.2	[29]
Oxidized carbon nanotubes	1.0	[30]
Ch/IA/MAA hydrogel	105.5	Present study

[a] pH 8, probably precipitation takes place.

Table 4
The influence of desorbing agents on the desorption efficiency of Zn(II) from the zinc-loaded Ch/IA/MAA-3 hydrogel.

Desorbing agent	Desorption efficiency (%)
0.01 M HNO_3	100.0
0.1 M HNO_3	100.0
0.01 M CH_3COOH	50.3
0.1 M CH_3COOH	100.0

a relatively rough surface morphology in the case when Zn^{2+} ions are absorbed from more concentrated solutions, as can be seen from the topography AFM image given in Fig. 7e. Details of such zinc containing phase can be seen in a corresponding phase image given in Fig. 7f, which shows only grainy structure with no flat domains.

Adsorption capacities of different sorbents, reported recently in the literature, are included in Table 3 along with the values obtained in this study. Obviously, the Ch/IA/MAA-3 hydrogel exhibits higher adsorption capacity. Apart from the adsorption on the surface of the hydrogel, sorption takes place in the bulk, as confirmed by SEM/EDX analysis and AFM surface topography and phase images.

3.5. Desorption studies

Consecutive sorption-desorption cycles were conducted to explore the potential of reusability of the hydrogels and recovery of metal ions. The sorption/desorption cycles were repeated for three times using 0.035 g of the sorbent and 660 mg/L of Zn^{2+} ion solution in total volume of 50 mL. Desorption was done with HNO_3 and CH_3COOH (mass of loaded sorbent 0.035 g; volume of solution 50 mL, concentration 0.01 and 0.1 mol/L; duration of process 24 h). The solution was analyzed for desorbed Zn^{2+} ions using ICP-MS. Both HNO_3 solutions, 0.1 mol/L and 0.01 mol/L, appeared to be effective for zinc ion desorption (100.0%), Table 4. The 0.01 mol/L HNO_3 solution was used in further sorption/desorption studies. The adsorption capacities did not show any significant decrease after the third reuse cycle.

4. Conclusions

In this study, pH-sensitive hydrogels based on chitosan, itaconic acid and methacrylic acid were used as a sorbent for removal of Zn^{2+} ions from aqueous solution. Solution pH and temperature had significant effect on the Zn^{2+} ion sorption since they had influence to the properties of hydrogels, as well as to the sorption process.

Kinetic studies show that experimental data can be described by the pseudo-second order kinetic for both hydrogels, Ch/IA/MAA-1 and Ch/IA/MAA-3. FTIR spectra of these hydrogels indicated that $-NH_2$, $-OH$ and $-COOH$ groups were all involved in the adsorption process. On the basis of the results obtained, three examined Ch/IA/MAA hydrogels could be considered as a potential sorbent for Zn^{2+} ion removal from aqueous solution, but Ch/IA/MAA-3 hydrogel was the most efficient.

The Langmuir and Redlich–Peterson isotherm model were found to fit the equilibrium adsorption data on Ch/IA/MAA-3 hydrogel well, while the values of Gibbs free energy change indicated that the process is spontaneous. Even it was concluded that the process is exothermic because of negative ΔH, an increase in temperature resulted in improved sorption performance due to the higher degree of swelling of hydrogel at elevated temperatures. The value obtained for maximum sorption capacity of 105.5 mg/g at 25 °C, is higher in comparison with other sorbents reported recently in literature. The hydrogel can be regenerated with 0.01 mol/L HNO_3.

References

[1] R.M.M. Sampaioa, R.A. Timmersa, N. Kocksa, V. Andréb, M.T. Duarteb, E.D. van Hullebuschc, F. Fargesd, P.N.L. Lensa, Zn–Ni sulfide selective precipitation: the role of supersaturation, Sep. Purif. Technol. 74 (2010) 108–118.
[2] M. Arora, B. Kiran, S. Rani, A. Rani, B. Kaur, N. Mittal, Heavy metal accumulation in vegetables irrigated with water from different sources, Food Chem. 111 (2008) 811–815.
[3] Institute of Medicine, Food and Nutrition Board, Dietary Reference Intakes for Vitamin A, Vitamin K, Arsenic, Boron, Chromium, Copper, Iodine, Iron, Manganese, Molybdenum, Nickel, Silicon, Vanadium, and Zinc, National Academy Press, Washington, D.C., 2001.
[4] M.F.M. Bijmans, P.-J. van Helvoort, C.J.N. Buisman, P.N.L. Lens, Effect of the sulfide concentration on zinc bio-precipitation in a single stage sulfidogenic bioreactor at pH 5.5, Sep. Purif. Technol. 69 (2009) 243–248.
[5] A. Belén Pérez Marín, M. Isabel Aguilar, J. Francisco Ortuño, V. Francisco Meseguer, J. Sáez, M. Lloréns, Biosorption of Zn(II) by orange waste in batch and packed-bed systems, J. Chem. Techol. Biotechnol. 85 (2010) 1310–1318.
[6] N. Gupta, S.S. Amritphale, N. Chandra, Removal of Zn (II) from aqueous solution by using hybrid precursors of silicon and carbon, Bioresour. Technol. 101 (2010) 3355–3362.
[7] Dj. Stojakovic, J. Hrenovic, M. Mazaj, N. Rajic, On the zinc sorption by the Serbian natural clinoptilolite and the disinfecting ability and phosphate affinity of the exhausted sorbent, J. Hazard. Mater. 185 (2010) 408–415.
[8] S. Nii, S. Okumura, T. Kinoshita, Y. Ishigaki, K. Nakano, K. Yamaguchi, S. Akita, Extractant-impregnated organogel for capturing heavy metals from aqueous solutions, Sep. Purif. Technol. 73 (2010) 250–255.
[9] R. Malberg, I. Dékány, G. Lagaly, Short chain alkylammonium montmorillonites and alcohols: gas adsorption and immersional wetting, Clay Miner. 24 (1989) 631–647.
[10] F. Berger, I. Dékány, K. Beneke, G. Lagaly, Selective liquid sorption and wetting on pillared montmorillonite, Clay Miner. 32 (1997) 331–339.
[11] I. Dékány, L. Túri, G. Galbács, J.H. Fendler, Cadmium ion adsorption controls the growth of CdS nanoparticles on layered montmorillonite and calumite surfaces, J. Colloid Interface Sci. 213 (1999) 584–591.
[12] I. Dékány, V. Seefeld, G. Lagaly, Time dependent changes of adsorption and wetting properties of pillared montmorillonites, Clay Miner. 35 (2000) 763–769.
[13] A. Farkas, I. Dékány, Interlamellar adsorption of organic pollutants in hydrophobic montmorillonite, Colloid Polym. Sci. 279 (2001) 459–467.
[14] T. Pernyeszi, I. Dékány, Photocatalytic degradation of hydrocarbons by montmorillonite and TiO2 in aqueous suspensions containing surfactants, Colloids Surf. A 230 (2003) 191–199.
[15] Y. Özdemir, M. Doğan, M. Alkan, Adsorption of cationic dyes from aqueous solutions by sepiolite, Microporous Mesoporous Mater. 96 (2006) 419–427.
[16] Y. Shu, L. Li, Q. Zhang, H. Wu, Equilibrium, kinetics and thermodynamic studies for sorption of chlorobenzenes on CTMAB modified bentonite and kaolinite, J. Hazard. Mater. 173 (2010) 47–53.
[17] M.M. Akafia, T.J. Reich, C.M. Kortesky, Assessing Cd, Co, Cu, Ni and Pb sorption on montmorillonite using surface complexation models, Appl. Geochem. 26 (2011) S154–S157.
[18] S. Lazarević, I. Janković-Častvan, Ž. Radovanović, B. Potkonjak, Dj. Janaćković, R. Petrović, Sorption of Cu2+ and Co2+ from aqueous solutions onto sepiolite: an equilibrium, kinetic and thermodynamic study, J. Serb. Chem. Soc. 76 (2011) 101–112.
[19] B.I. Olu-Owolabi, E.I. Unuabonah, Kinetic and thermodynamics of the removal of Zn2+ and Cu2+ from aqueous solution by sulphate and phosphate-modified bentonite clay, J. Hazard. Mater. 184 (2010) 731–738.
[20] T. Kanti Sen, D. Gomez, Adsorption of zinc (Zn2+) from aqueous solution on natural bentonite, Desalination 267 (2011) 286–294.
[21] N.B. Milosavljević, N.Z. Milašinović, I.G. Popović, J.M. Filipović, M.T. Kalagasidis Krušić, Preparation and characterization of pH-sensitive hydrogels based on chitosan, itaconic and methacrylic acid, Polym. Int. 60 (2011) 443–452.

[22] N.B. Milosavljević, M.Đ. Ristić, A.A. Perić-Grujić, J.M. Filipović, S.B. Štrbac, Z.Lj. Rakočević, M.T. Kalagasidis Krušić, Hydrogel based on chitosan, itaconic acid and methacrylic acid as adsorbent of Cd^{2+} ions from aqueous solution, Chem. Eng. J. 165 (2010) 554–562.

[23] A. Kaya, A.H. Oren, Adsorption of zinc from aqueous solutions to bentonite, J. Hazard. Mat. B 125 (2005) 183–189.

[24] S. Kocaoba, Y. Orhan, T. Akyüz, Kinetics and equilibrium studies of heavy metal ions removal by use of natural zeolite, Desalination 214 (2007) 1–10.

[25] S.S. Lagergren, Zur theorieder sogennanten adsorption gelöster stoffe, K. Sven. Vetenskapsakad. Handl. 24 (1988) 1–39.

[26] Y.S. Ho, G. MsKay, Pseudo-second order model for adsorption processes, Process Biochem. 34 (1999) 451–465.

[27] A. Ramesh, D.J. Lee, J.W.C. Wong, Thermodynamic parameters for adsorption equilibrium of heavy metals and dyes from wastewater with low-cost adsorbents, J. Colloid Interface Sc. 291 (2005) 588–592.

[28] U. Yildiz, Ö.F. Kemik, B. Hazer, The removal of heavy metal ions from aqueous solutions by novel pH-sensitive hydrogels, J. Hazard. Mater. 183 (2010) 521–532.

[29] M.A. Sharaf, H.A. Arida, S.A. Sayed, A.A. Younis, A.B. Farag, Separation and preconcentration of some heavy-metal ions using new chelating polymeric hydrogels, J. Appl. Polym. Sci. 113 (2009) 1335–1344.

[30] Z. Gao, T.J. Bandosz, Z. Zhao, M. Han, J. Qiu, Investigation of factors affecting adsorption of transition metals on oxidized carbon nanotubes, J. Hazard. Mater. 167 (2009) 357–365.